Horizon 2020
European Union funding
for Research & Innovation

Horizon 2020 Grant Agreement Number 734798

indoor small-cell Networks with 3D MIMO Array Antennas (is3DMIMO)

D2.1
Single and Array Antennas Designs for Millimeter-Wave Applications

Authors(s)	Sadegh Mansouri Moghaddam, Andrés Alayón Glazunov, Jian Yang, and Yang Wang
Author(s) Affiliation	Department of Electrical Engineering, Chalmers University of Technology, Gothenburg, Sweden; Harbin Institute of Technology, Shenzhen Graduate School, China.
Editor(s):	Andrés Alayón Glazunov
Status-Version:	Final-1.0
Project Number:	734798
Project Title:	indoor small-cell Networks with 3D MIMO Array Antennas (is3DMIMO)
Project Acronym:	is3DMIMO
Work Package Number	2

Abstract In the past few years, the ever increasing need for high data-rate communications has drawn lots of attention towards the millimeter-wave (mm-wave) frequencies due to the availability of large chunks of bandwidth. The applications are many, e.g., high resolution imaging and wireless communications over short distance at the V-band (60 GHz), but also over longer ranges at $20-40$ GHz, suitable for 5G wireless. Therefore, ultra-wideband (UWB) wide-scan phased array antennas easily integrated with active components at a low manufacturing cost become a necessity. To provide the suitable antenna for the mm-wave application, we propose an ultra-wideband antenna for mm-wave applications. The antenna consists of a bowtie patch integrated with the feeding network. The feeding network is implemented as a multilayer substrate structure. The simulated antenna shows a relative bandwidth of $2.6:1$ with a reflection coefficient better than -8 dB. The radiation pattern remains fairly stable over $20-50$ GHz with a boresight directivity of $5.8-8.3$ dBi. Using the proposed configuration, we present a dual-polarized ultra-wideband element in an infinite large array condition for planar phased array antennas in mm-wave applications. The array antenna consists of tightly-coupled bowties in a dual-offset configuration. In order to simplify the manufacturing process and eliminate the scalability limitation, a new feeding network is employed. The feeding is inspired by magneto-electric dipoles (MEDs) and planar ultra-wideband array antennas (PUMAs). Hence, the feeding is integrated with the horizontally oriented radiating bowties and removes the need for the external baluns. The simulated antenna shows relative bandwidths of $2.3:1$ and $3:1$ at VSWR<3, for maximum scanning angles of 60° and 45°, respectively, at both E- and H-planes.
The results summarized in this deliverable have been presented as conference papers [1,2]. The antenna designs and concepts are related to Task 2.1, where we have looked into the millimeter wave frequencies. The results of this deliverable lay the ground to work produced in Task 2.1 and is the input to work produced Task 2.2, Task 1.2 and Task 1.3.

Keywords: Wideband antenna, Array antenna, UWB, mm-Wave, Phased array antenna.

Table of Contents

Index of Figures

1 Introduction

The growing demand on high data-rate communication has called for the millimeter-wave (mm-wave) frequency bands. 5G cellular communications at $20-60$ GHz, short-distance low-interference back-haul applications at V-band (60 GHz) and high data-rate satellite communication at E and W bands ($70-110$ GHz) are some examples illustrating the importance of the mm-wave technology [3, 4]. In order to support multiple bands, especially for cellular applications, antennas with ultra-wide bandwidths (UWB) are preferred. Also, the antennas should be easily integrated with active and passive components as well as fabricated by simple manufacturing process.

Ultra-wideband (UWB), wide-scanning and dual-polarized phased array antennas offer multi-channel and multi-function configurations with the ability to electronically scan the beam. Different array antenna configurations have been suggested in the literature to produce the desired performance. Tapered-slot arrays can provide a large bandwidth of 10:1 [5]. However, these antennas are relatively bulky and difficult to assemble. Planar dipoles are low-profile and versatile candidates. Using the Wheeler's current sheet [6], tightly-coupled dipoles above the ground plane can provide a relatively large bandwidth of 9:1 [7]. However, these arrays need a wideband balun for each element to sustain their performance. In [8–10], tightly-coupled dipoles are used together with a passive Marchand baluns. To eliminate the complexity of the external balun, planar ultra-wideband modular arrays (PUMAs) are proposed in [11,12]. PUMAs are planar structures with an integrated feeding network which can be manufactured by using simple multilayer PCB. Because of the integration of the feed, the need to have an external balun is eliminated in these antennas. Another example of wideband antennas with integrated feeding network are the Magneto-Electric Dipoles (MED) [13–15]. However, these antennas are mostly considered for single-antenna structures.

All the above-mentioned UWB arrays will face the scalability problem in terms of manufacturing and assembling as we move up to higher mm-wave frequencies. Although, there are many array antennas designed for these frequency bands, most of them are relatively narrow band [16] or require a more complex and expensive manufacturing process [17]. In [18], a single-polarized low-cost UWB mm-wave antenna is suggested using a multilayer tightly-coupled dipole element. While providing wideband characteristics, this structure is very close to the limit of the PCB manufacturing capabilities and needs to be modified to provide more reliability.

In this deliverable, we propose an UWB bowtie antenna for mm-wave applications. The design is comprised of a planar bowtie integrated with the feeding network. The

integration of the feeding network to the bowtie has been accomplished by using multilayer PCB and via holes. Using the above mentioned concept, a dual-polarized UWB mm-wave array antenna is presented. One can see the resemblance of the proposed structure to the tightly-coupled dipoles fed with Marchand baluns, the MEDs and the PUMAs.

The work presented here will be used in future work that will lead to publications related to Tasks 2.1, 2.2, 1.2 and 1.3.

2 Single Bowtie Antenna

2.1 Antenna Design

Fig. 1 shows the geometry of the proposed antenna. It consists of a bowtie above a large ground plane. The ground plane helps the antenna to achieve a directional radiation pattern. A row of five vertical vias connects each petals of the bowtie to the ground plane. To excite the antenna, a Γ-shaped probe is employed, i.e., a similar method used to excite MEDs. The feeding probe has three different parts. The first vertical part is implemented by a via hole and is fed below the ground plane, through a 50Ω coaxial cable. This part, together with the row of via holes, transfers the fields to the second part of the Γ-shaped probe which is horizontally oriented. This is where the excitation of the grounded bowtie structure occurs. The length of this part and the third vertically oriented part of the probe, which acts as an open transmission line, can compensate each other to achieve a good impedance matching. One can also see the similarity of this design to the design of planar dipoles integrated with Marchand baluns.

The final structure has three layers. $RogersRT5880$ with dielectric constant of 2.2 is used as substrate. The diameter of via holes are 0.2 mm to comply with manufacturing precision limitations. The total height of the antenna is 1.26 mm and the size of the ground plane is 12×12 mm^2.

2.2 Simulated Results

CST Microwave Studio has been used for electromagnetic simulations. The simulated reflection coefficient of three different types of excitations are compared in Fig. 2. First, we excite the bowtie by a discrete port with impedance of 150 Ω. The second curve, represents the bowtie antenna excited by 150 Ω discrete port, including two rows of via holes. Finally, we compare these two ideally excitations with a practical feeding structure, using the Γ-shaped probe. We can see that the reflection coefficient is below -8 dB over the frequency band of $22 - 57$ GHz.

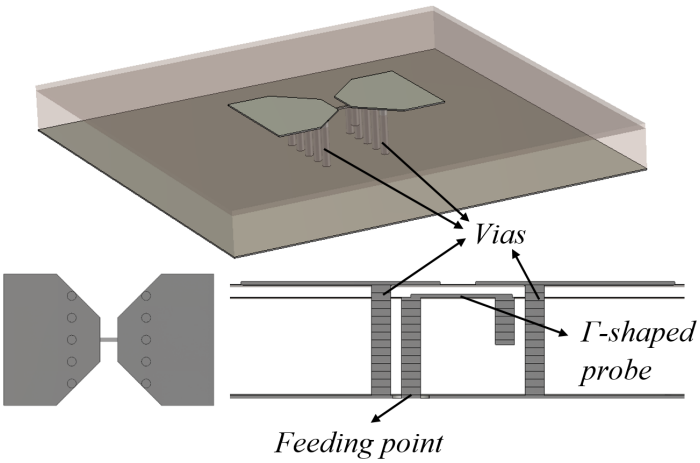

Figure 1: The proposed antenna structure.

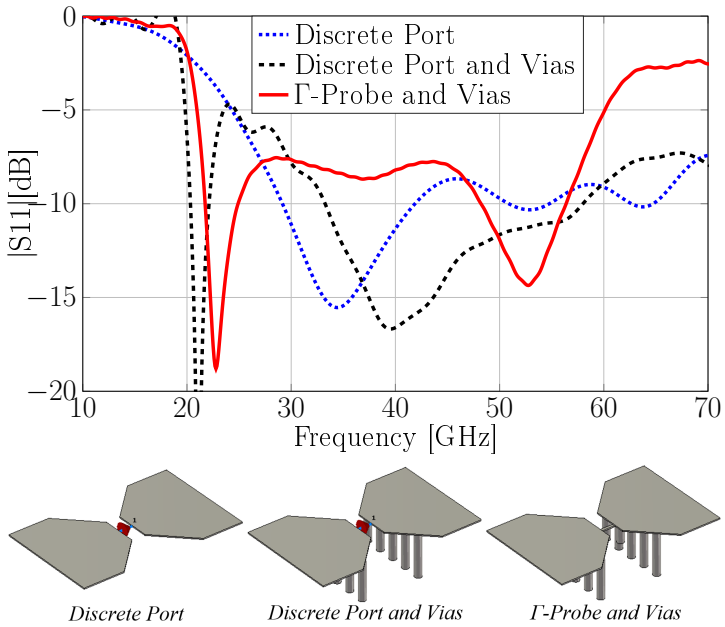

Figure 2: The comparison of the reflection coefficient for three different excitations.

Fig. 3 illustrates the boresight directivity of three different excitations. As can be seen, the stability of the boresight directivity can be increased by adding the rows of via holes. Also we can see that the directivity is almost the same for structures comprised of bowties and vias, when the discrete port excitation is implemented by Γ-shaped probe.

The simulated radiation patterns of the antenna in 45°-plane (D-plane) at three different frequencies are shown in Fig. 4. We see that the radiation pattern is stable over $20 - 50$ GHz. Also, the symmetry in co-polar and cross-polar components of the radiation pattern implies the good performance of the feeding network to excite the bowtie, differentially.

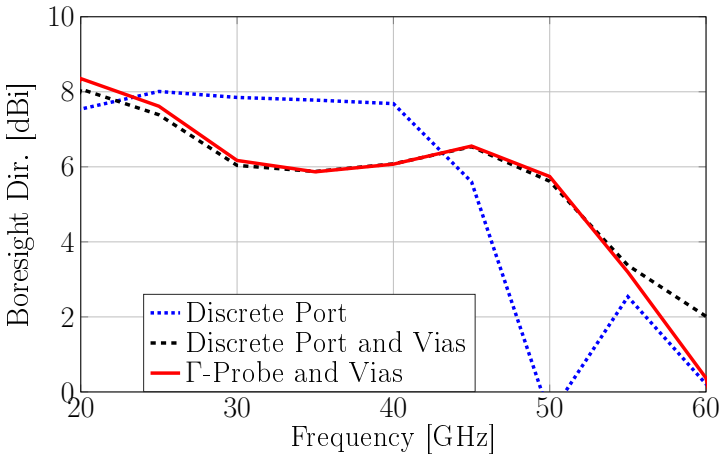

Figure 3: The comparison of the boresight directivity for three different excitations.

3 Dual-Polarized Array Antenna

3.1 Element Design

The element is comprised of a planar dipole or bowtie fed by means of via holes in a tightly-coupled dual-offset configuration (Fig. 5). The bowtie element is placed approximately $\lambda_{mid}/4\sqrt{\epsilon_r}$ above the ground plane where ϵ_r is the relative permittivity of Rogers RT5880 which has been used as substrate and λ_{mid} is the wavelength at the middle frequency of the band. This tightly-coupled configuration can exhibit wideband impedance characteristics

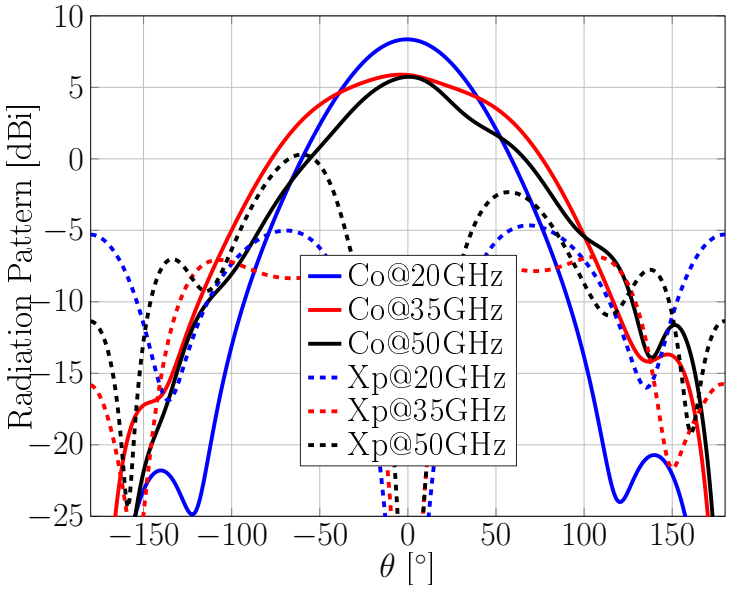

Figure 4: The radiation pattern of the proposed antenna in 45°-plane (D-plane), at three different frequencies of 20 GHz, 35 GHz and 50 GHz.

[19], utilizing the current sheet principle. Also, a dielectric layer of the same substrate is placed on top of the array to further improve the impedance matching [7].

In order to excite each element in tightly-coupled arrays, an external balun needs to be designed. In [20], it is shown that the ideally fed tightly-coupled arrays can achieve a $4:1$ bandwidth with VSWR< 2. However, the lack of shielding of the feed lines can restrict the scanning along the E-plane [11].

In Fig. 5(c) a cross-sectional view at a cutting plane in the middle of the element is illustrated. As can be seen, a Γ-shaped probe has been used to feed the element, similar to MEDs. Plated vias are employed to transfer the field to the horizontal part of the Γ-probe. The vertically oriented open ending part of the probe is employed to adjust the matching impedance. The positions of the shorting vias can also define the low frequency characteristics. Also, they can shield the feed lines and prevent the E-plane scanning problem mentioned earlier.

The probe is fed below the ground plane by a 75 Ω coaxial cable. Shorting vias have a diameter equal to 0.1 mm. The size of the element is set to 1.3 mm to prevent the appearance of grating lobes, while scanning up to $\theta = 60°$ at 110 GHz. The structure can be fabricated as a multilayer PCB, while the feed lines and shorting posts are implemented as via holes.

3.2 Simulated Results

The unit cell has been simulated in an infinite boundary condition using Ansoft HFSS. Fig. 6 shows the VSWR for different scan angles up to 60° at E- and H-planes. As can be seen, for scanning up to $\theta = 60°$ a VSWR lower than 3 is achieved over the frequency band of $44 - 100$ GHz at both E- and H-planes. However, for the scan angle of $\theta = 45°$ at both basic planes, the covered frequency band for the same VSWR will increase to $36 - 110$ GHz.

In Fig. 7 and Fig. 8, the corresponding scattering parameters at three different frequencies are illustrated. The horizontal polarization is considered for these results. This corresponds to the scanning in E-plane when $\phi = 0°$ and in H-plane when $\phi = 90°$. In Fig. 7, we can see that the values of S_{11} at other planes, lies withing the values of S_{11} at these basic planes. On the other hand, the maximum coupling happens at $\phi = 45°$ (D-plane). As shown in Fig. 8, a coupling better than -13 dB is seen when the array scans up to $\theta = 60°$. However, it improves to -20 dB when the scanning angle reduces to $\theta = 45°$. It needs to be mentioned that because of the symmetry, both polarizations will show the same results.

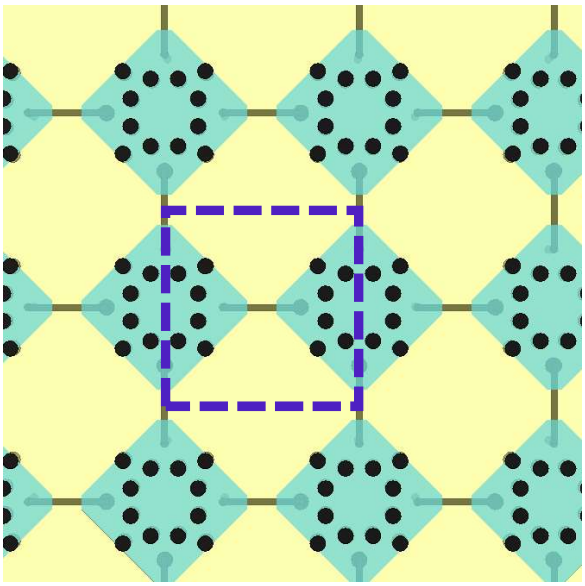

(a)

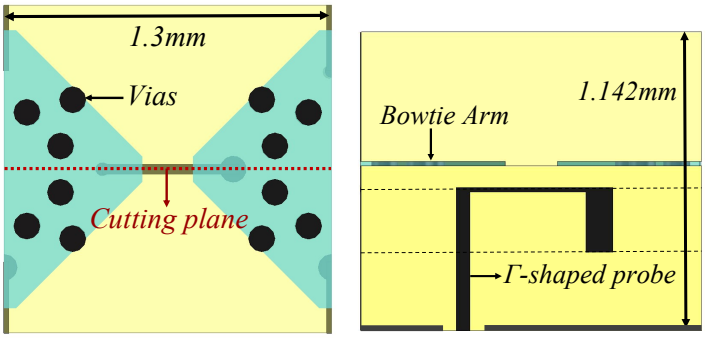

(b) (c)

Figure 5: The geometry of the proposed antenna. a) Top view of the array, showing the bowtie layer, shorting posts and feed lines b) Top view of the unit cell and c) cross-sectional view of the unit cell at the cutting plane showing the Γ-shaped probe.

4 Conclusion

In this deliverable, we have presented an ultra-wideband bowtie structure suitable for mm-wave applications. The feeding mechanism of the proposed antenna is an integrated feeding network, implemented by multilayer PCB and via holes. The bandwidth of 2.6 : 1 was achieved in terms of reflection coefficient better than -8 dB for the single antenna. The radiation pattern was stable and the directivity was between $5.8 - 8.3$ dBi over the frequency band of $20 - 50$ GHz. The antenna can further be optimized to achieve better performance, considering the manufacturing limitation. Also, we have presented a

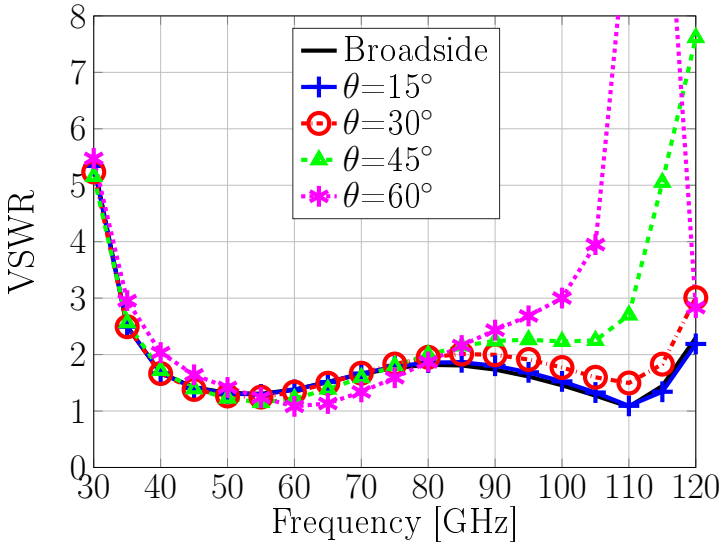

(a)

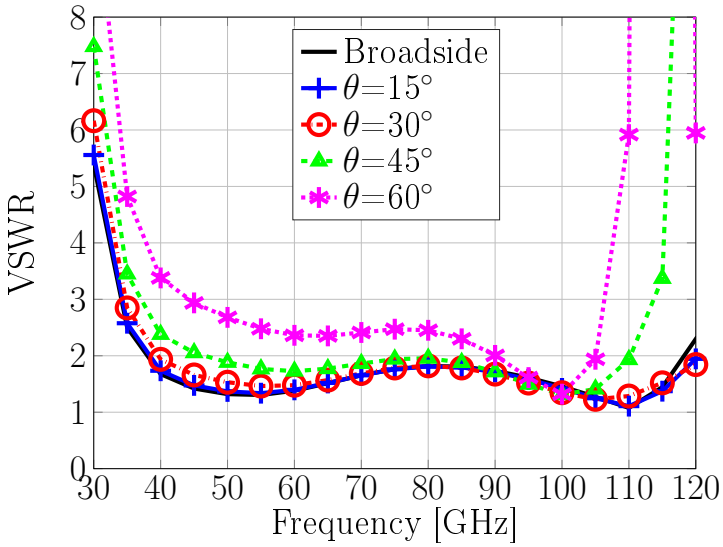

(b)

Figure 6: Simulated active VSWR versus frequency for different scanning angles at a) E-plane and b) H-plane.

dual-polarized ultra-wideband element in an infinite array environment for phased array antenna for mm-wave applications. The element was based on tightly-coupled dipoles together with an integrated feeding network. The feeding integration was employed using plated vias which eliminated the need for an external balun. This resulted in a planar structure which can be fabricated using multilayer PCB. Dual-polarization was implemented by using dual-offset configuration. The relative bandwidth of 2.3:1 has been achieved in terms of VSWR < 3 for the scanning up to $\theta = 60°$. By limiting the scanning

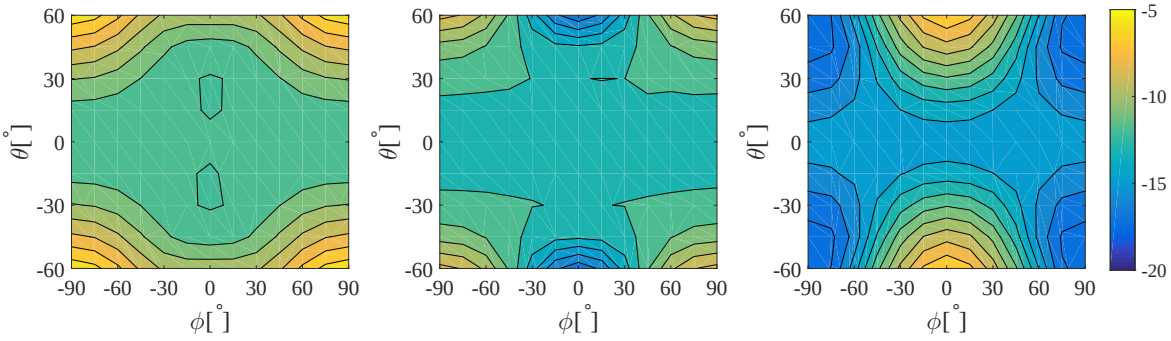

(a) (b) (c)

Figure 7: The simulated active reflection coefficient (S_{11}) for the scanning up to $\theta = 60°$ at a) 40 GHz b) 70 GHz and c) 100 GHz.

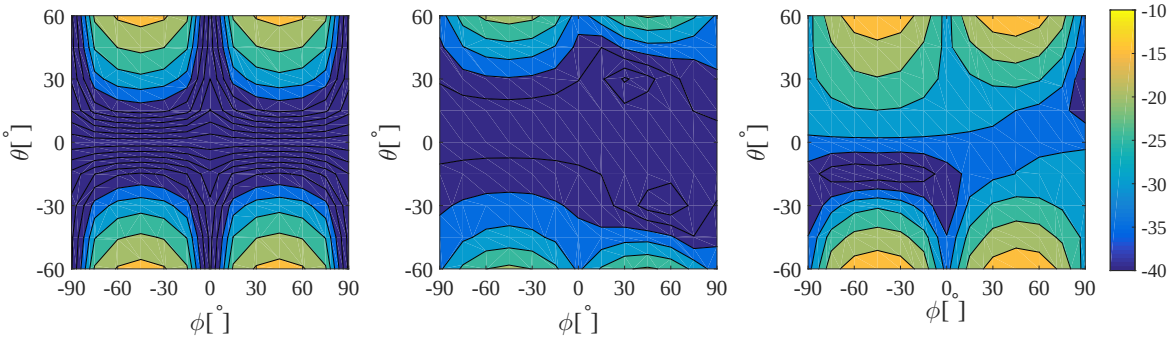

(a) (b) (c)

Figure 8: The simulated active coupling (S_{21}) between the two orthogonal polarizations for the scanning up to $\theta = 60°$ at a) 40 GHz b) 70 GHz and c) 100 GHz.

angle to $\theta = 45°$, we have seen that the relative bandwidth increased to 3:1. An isolation between the orthogonal ports better than 13 dB and 20 dB has been achieved for $\theta = 60°$ and $\theta = 45°$, respectively.

In this deliverable we have presented the necessary groundwork to produce optimized array antennas for 3D Spatial Multiplexing (SMX) and 3D Beamforming that are parts of Task 2.1.

References

[1] S. M. Moghaddam, J. Yang, and A. A. Glazunov, "Ultra-wideband millimeter-wave bowtie antenna," in *Antennas and Propagation (ISAP), 2017 International Symposium*. IEEE, 2017, pp. 1–2.

[2] ——, "A planar dual-polarized ultra-wideband millimeter-wave array antenna," in *Antennas and Propagation (EUCAP), 2018 12th European Conference on.* IEEE, 2018.

[3] J. G. Andrews, S. Buzzi, W. Choi, S. V. Hanly, A. Lozano, A. C. Soong, and J. C. Zhang, "What will 5g be?" *IEEE Journal on selected areas in communications*, vol. 32, no. 6, pp. 1065–1082, 2014.

[4] P. Smulders, "Exploiting the 60 ghz band for local wireless multimedia access: Prospects and future directions," *IEEE communications magazine*, vol. 40, no. 1, pp. 140–147, 2002.

[5] S. S. Holland and M. N. Vouvakis, "The banyan tree antenna array," *IEEE Transactions on Antennas and Propagation*, vol. 59, no. 11, pp. 4060–4070, 2011.

[6] H. Wheeler, "Simple relations derived from a phased-array antenna made of an infinite current sheet," *IEEE Transactions on Antennas and Propagation*, vol. 13, no. 4, pp. 506–514, 1965.

[7] B. Munk, R. Taylor, T. Durharn, W. Croswell, B. Pigon, R. Boozer, S. Brown, M. Jones, J. Pryor, S. Ortiz *et al.*, "A low-profile broadband phased array antenna," in *Antennas and Propagation Society International Symposium, 2003. IEEE*, vol. 2. IEEE, 2003, pp. 448–451.

[8] J. P. Doane, K. Sertel, and J. L. Volakis, "A wideband, wide scanning tightly coupled dipole array with integrated balun (tcda-ib)," *IEEE Transactions on Antennas and Propagation*, vol. 61, no. 9, pp. 4538–4548, 2013.

[9] P. Lindberg, E. Ojefors, Z. Barna, A. Thornell-Pers, and A. Rydberg, "Dual wideband printed dipole antenna with integrated balun," *IET microwaves, antennas & propagation*, vol. 1, no. 3, pp. 707–711, 2007.

[10] J. Doane, K. Sertel, and J. Volakis, "A wideband scanning conformal array with a compact compensating balun," in *Antenna Applications Symposium*, 2012.

[11] S. S. Holland and M. N. Vouvakis, "The planar ultrawideband modular antenna (puma) array," *IEEE Transactions on Antennas and Propagation*, vol. 60, no. 1, pp. 130–140, 2012.

[12] S. S. Holland, D. H. Schaubert, and M. N. Vouvakis, "A 7–21 ghz dual-polarized planar ultrawideband modular antenna (puma) array," *IEEE Transactions on Antennas and Propagation*, vol. 60, no. 10, pp. 4589–4600, 2012.

[13] K.-M. Luk and H. Wong, "A new wideband unidirectional antenna element," *Int. J. Microw. Opt. Technol.*, vol. 1, no. 1, pp. 35–44, 2006.

[14] L. Siu, H. Wong, and K.-M. Luk, "A dual-polarized magneto-electric dipole with dielectric loading," *IEEE Transactions on antennas and propagation*, vol. 57, no. 3, pp. 616–623, 2009.

[15] B. Q. Wu and K.-M. Luk, "A broadband dual-polarized magneto-electric dipole antenna with simple feeds," *IEEE Antennas and Wireless Propagation Letters*, vol. 8, pp. 60–63, 2009.

[16] G. Rankin, A. Tirkel, and A. Leukhin, "Millimeter wave array for uav imaging mimo radar," in *Radar Symposium (IRS), 2015 16th International*. IEEE, 2015, pp. 499–504.

[17] T. E. Durham, K. J. Vanhille, C. R. Trent, K. M. Lambert, and F. A. Miranda, "Design of an 8–40 ghz antenna for the wideband instrument for snow measurements (wism)," in *Antennas and Propagation & USNC/URSI National Radio Science Meeting, 2015 IEEE International Symposium on*. IEEE, 2015, pp. 1999–2000.

[18] M. H. Novak, J. L. Volakis, and F. A. Miranda, "Low cost ultra-wideband millimeter-wave array," in *Antennas and Propagation (APSURSI), 2016 IEEE International Symposium on*. IEEE, 2016, pp. 1841–1842.

[19] D. Staiman, M. Breese, and W. Patton, "New technique for combining solid-state sources," *IEEE Journal of Solid-State Circuits*, vol. 3, no. 3, pp. 238–243, 1968.

[20] B. A. Munk, *Finite antenna arrays and FSS*. John Wiley & Sons, 2003.